Science of the Total Environment 912 (2024) 169201

Contents lists available at ScienceDirect

Science of the Total Environment

journal homepage: www.elsevier.com/locate/scitotenv

Light and temperature controls of aquatic plant photosynthesis downstream of a hydropower plant and the effect of plant removal

Benoît O.L. Demars [a,*], Susanne C. Schneider [a], Kirstine Thiemer [a], Peter Dörsch [b], Ulrich Pulg [c], Sebastian Stranzl [c], Gaute Velle [c,d], Devanshi Pathak [e]

[a] *Norwegian Institute for Water Research (NIVA), Økernveien 94, 0579 Oslo, Norway*
[b] *Faculty of Environmental Sciences and Natural Resource Management, Norwegian University of Life Sciences, 1432 Ås, Norway*
[c] *Norwegian Research Centre, Nygårdsgaten 112, 5008 Bergen, Norway*
[d] *Department of Biological Sciences, University of Bergen, Thormøhlensgate 53 A & B, 5006 Bergen, Norway*
[e] *Department Aquatic Ecosystem Analysis (ASAM), Helmholtz Centre for Environmental Research – UFZ, Brückstr. 3a, 39114 Magdeburg, Germany*

HIGHLIGHTS

- Regulated rivers can lead to mass development of aquatic plants.
- Mechanical harvesting is often used to remove aquatic plants, seen as invasive.
- Whole stream metabolism provided daily aquatic plant photosynthesis over an annual cycle.
- Effect of plant removal was predicted from models of plant photosynthesis and expansion.
- Intensity of mechanical harvesting constrained ecosystem resilience and carbon regulation.

GRAPHICAL ABSTRACT

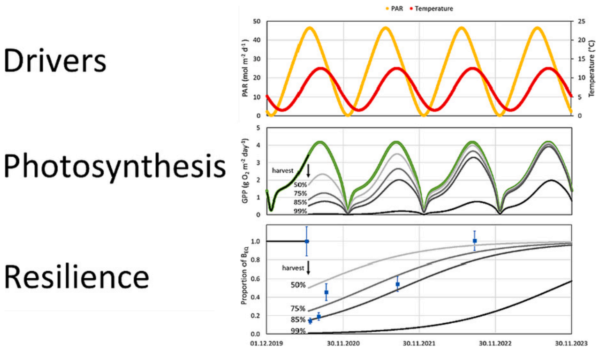

ARTICLE INFO

Editor: Sergi Sabater

Keywords:
Photosynthesis
Macrophyte removal
Regulated river
Metabolic theory
Light
Temperature
Resilience

ABSTRACT

Many rivers worldwide are regulated, and the altered hydrology can lead to mass development of aquatic plants. Plant invasions are often seen as a nuisance for human activities leading to costly remedial actions with uncertain implications for aquatic biodiversity and ecosystem functioning. Mechanical harvesting is often used to remove aquatic plants and knowledge of plant growth rate could improve management decisions. Here, we used a simple light-temperature theoretical model to make *a priori* prediction of aquatic plant photosynthesis. These predictions were assessed through an open-channel diel change in O_2 mass balance approach. A Michaelis-Menten type model was fitted to observed gross primary production (GPP) standardised at 10 °C using a temperature dependence from thermodynamic theory of enzyme kinetics. The model explained 87 % of the variability in GPP of a submerged aquatic plant (*Juncus bulbosus* L.) throughout an annual cycle in the River Otra, Norway. The annual net plant production was about 2.4 (1.0–3.8) times the standing biomass of *J. bulbosus*. This suggests a high continuous mass loss due to hydraulic stress and natural mechanical breakage of stems, as the biomass of *J. bulbosus* remained relatively constant throughout the year. *J. bulbosus* was predicted to be resilient to mechanical harvesting with photosynthetic capacity recovered within two years following 50–85 % plant removal.

---

[*] Corresponding author.
E-mail address: benoit.demars@niva.no (B.O.L. Demars).

https://doi.org/10.1016/j.scitotenv.2023.169201
Received 24 July 2023; Received in revised form 1 December 2023; Accepted 6 December 2023
Available online 9 December 2023
0048-9697/© 2023 The Authors. Published by Elsevier B.V. This is an open access article under the CC BY license (http://creativecommons.org/licenses/by/4.0/).

The predicted recovery was confirmed through a field experiment where 72 % of *J. bulbosus* biomass was mechanically removed. We emphasise the value of using a theoretical approach, like metabolic theory, over statistical models where *a posteriori* results are not always easy to interpret. Finally, the ability to predict ecosystem resilience of aquatic photosynthesis in response to varying management scenarios offers a valuable tool for estimating aquatic ecosystem services, such as carbon regulation. This tool can benefit the EU Biodiversity Strategy and UN Sustainable Development Goals.

1. Introduction

Large parts of the Earth's rivers are now highly fragmented and flow regulated (Nilsson et al., 2005; Grill et al., 2019). The removal of flood dynamics, through water transfer and retention in reservoirs, alters geomorphological processes and may promote the mass development of aquatic submerged plants (Gurnell, 2014; Riis and Biggs, 2003), even in oligotrophic rivers (Rørslett, 1988; Rørslett et al., 1989; Nilsson, 1978). The mass development of aquatic plants is a worldwide problem often seen as nuisance for human activities, such as boat traffic, swimming, fishing, hydropower and hydrological functioning of the system (Verhofstad and Bakker, 2019; Thiemer et al., 2023). Undesirable plant growth leads to costly remedial actions with variable effectiveness (Rørslett and Johansen, 1996; Hussner et al., 2017). Proliferation of plants can alter aquatic biodiversity and ecosystem functioning (Thiemer et al., 2021; Schultz and Dibble, 2012; Velle et al., 2022; Misteli et al., 2023). Mechanical harvesting is often used to remove aquatic plants and knowledge of plant regrowth rate and its main drivers could improve management decisions (Thiemer et al., 2021).

Whole stream metabolism, including primary production, is strongly controlled by flow regime and light availability (Bernhardt et al., 2022), also in regulated rivers (Hall Jr. et al., 2015). Primary production may be more constrained by flow regime than temperature through control on standing biomass (Junker et al., 2021). Thus, stream temperature is likely the second most important factor controlling primary production (Demars et al., 2016). Although it is hard to disentangle the role of temperature from light in natural rivers (Huryn et al., 2014), regulated rivers often modify the thermal regime independently of light availability, allowing the quantification of temperature's role (Hall Jr. et al., 2015). These primary drivers may also interact with nutrient availability (Cross et al., 2022), reciprocal trophic exchange between primary producers and decomposers (Demars et al., 2020) and top down control (Liess et al., 2009).

The temperature dependence of stream photosynthesis has previously been based on a thermodynamic theory of enzyme kinetics for systems at *steady state* (Demars et al., 2016). Essentially, the theory assumes that a single, rate-limiting 'master reaction' (here the fixation of CO_2 by Rubisco) describes the temperature reaction norm of individual organisms. Natural selection is assumed here to operate at the level of the genes, where enzymes evolved with different forms balancing thermal stability (loose to compact molecular scaffolding with warming) with conservation of function (Demars et al., 2016). The genotypes of a given enzyme have different thermal optima but the same probability of activity along the thermal gradient. Expected peak performance of photosynthesis of genotypes increases systematically with temperature according to the average activation energy of enzymes. The theory assumes no temperature compensation in the carboxylation reaction at community level (other mechanisms may be at play) – Demars et al., 2016. The theory further assumes that Rubisco density and community size structure and biomass are independent of temperature. The theory recognised the central role of physiological CO_2-concentrating mechanisms preventing photorespiration, limiting photosynthesis with warming (Allen et al., 2005). The apparent activation energy of aquatic ecosystem photosynthesis was found to be approximately 0.57 electron volts (eV) for temperatures ranging from 4 to 45 °C, reflecting the average activation energy of enzymatic reactions (Elias et al., 2014). It remains to show how the theory may be applied when the equilibrium is disturbed, *e.g.* following mechanical harvesting of aquatic plants.

Here, we test how the theoretical temperature dependence of stream photosynthesis constrains the photosynthesis of a perennial submerged plant with CO_2-concentration mechanism under varying light conditions throughout an annual cycle in a regulated river. More specifically, we used a novel method to estimate gross primary production (GPP) using an open channel diel oxygen mass balance (Pathak and Demars, 2023) and predicted daily GPP with a Michaelis-Menten GPP-light model combined with an Arrhenius temperature model (Gillooly et al., 2001). The model was parameterised *a priori* with the theoretical activation energy (Demars et al., 2016), rather than with an *a posteriori* empirical fit (Hall Jr. et al., 2015; Song et al., 2018). We demonstrate how the theory may be used to predict recovery in gross primary production following loss of plant biomass. Finally, we demonstrate the usefulness of our approach for both management and the quantification of aquatic ecosystem services necessary for the European Union (EU) Biodiversity Strategy and United Nations Sustainable Development Goals.

2. Material and methods

2.1. Study site

The River Otra is situated in southern Norway and flows from north to south through forests in an alpine landscape. The River Otra is extensively used for hydropower production with water reservoirs and water transfers (Wright et al., 2017; Rørslett, 1988). The studied section drains about 1900 km^2, mostly through Brokke hydropower plant, and discharge is heavily regulated with characteristic diel changes (hydropeaking) to accommodate demand in electricity (Wright et al., 2017).

The hydropower plant periodically discharges water highly supersaturated in dissolved gases posing risks to fish health (Stenberg et al., 2022; Lennox et al., 2022). Supersaturation is due to air entrainment in the secondary water intakes of the hydropower plant, which dissolved in the pressure tunnels. Supersaturation varies, depending on the water source (secondary stream intakes *versus* reservoirs), and hydraulic head mostly independent of discharge (Pulg et al., 2016a; Stenberg et al., 2022). Total dissolved gas (TDG) was recorded every 30 min in the effluent (deep open canal) of the hydropower plant with a Total Gas Analyzer 3.0 (Fisch- und. Wassertechnik; Pulg et al., 2016a; Pulg et al., 2016b), based on the Weiss-saturometer principle (Weiss, 1970). The Gas Analyzer measures TDG pressure in a submerged gas-permeable silicon hose connected to an underwater pressure sensor and an atmospheric pressure sensor above the water surface. The saturation is measured as the gas pressure in the water relative to ambient air pressure. The relationship is shown as percentage, where values over 100 % indicate TDG supersaturation. The saturometer has an accuracy of ±10 hPa, which is approximately ±1 % TDG. The data were interpolated at 15 min intervals, including the short periods for which we had missing data (Pulg et al., 2022).

The studied river reach Rysstad – Straume (Fig. 1) shows profuse growth of the perennial aquatic plant *Juncus bulbosus* L. 3 to 7.8 km kilometres downstream of the hydropower plant effluent (Rørslett, 1988). Plant growth was favoured by water regulation since the 1960s and the installation of Tjurrmo dam at Hekni in the 1990s (3 km downstream of Straume). The natural bed slope of the river section Rysstad – Straume was subsequently changed from 0.0012 (0.12 %) to 0.0001 (0.01 %). We estimated plant cover (point recording along transects) and biomass (roots and shoots) within *J. bulbosus* patches (0.12 m^2 quadrats) in summer 2020 and inferred from the product an average (±se) standing biomass of 57 ± 8 g C m^{-2} over the whole study site. The CO_2 concentrations in the water column (20–60 μM CO_2 L^{-1}) were well below the level necessary to saturate underwater photosynthesis of the leaf apparatus of *J. bulbosus* (over 500 μM CO_2 L^{-1}, Sand-Jensen, 1987; Roelofs et al., 1984). However, *J. bulbosus* has an efficient internal gas recycling and CO_2 root uptake could partly alleviate CO_2 limitation (Wetzel et al., 1984; Wetzel et al., 1985) with sediment pore water concentrations averaging 170 μM CO_2 L^{-1} (Moe and Demars, 2017). The gas supersaturation at the outlet of the hydropower plant did not increase the partial pressure of CO_2 or photosynthesis in the studied reach (Demars and Dörsch, 2023). Most importantly, the physiology of the aquatic plant corresponded to the assumption of our thermodynamic theory of enzyme kinetics, *i.e.* the presence of a CO_2-concentration mechanism limiting photorespiration (Demars et al., 2016).

A monitoring station placed at Straume (Fig. 1) logged dissolved oxygen and water temperature at 15-min intervals (Xylem-Andeeraa optode 4831), as well as photosynthetic active radiation (PAR) above the water surface (LICOR, Quantum LI190R-L), air temperature and atmospheric pressure (Barometer RM Young 061302 V) using a Campbell datalogger (CR1000X). The oxygen sensor was inserted in a white plastic pipe at about 1 m depth fixed to Straume bridge and protruding into the main current. An additional oxygen optode (miniDOT PME, also recording temperature) was fixed on a post mid-column in the main water current at the top of the reach (Rysstad, Fig. 1). The oxygen optodes were cross calibrated in river water with saturated air using an air bubbler in a small tank by the side of the river, as in previous studies (*e.g.* Demars, 2019).

Hourly discharge data were available from the hydropower company just downstream the hydropower plant effluent (Brokke) and 11 km downstream at Hekni dam (Fig. 1). Discharge was interpolated at 15 min time intervals.

2.2. Estimation of aquatic plant photosynthesis

Since submerged *J. bulbosus* covered a large part of the sandy river bed (river section Rysstad-Straume, Fig. 1), plant photosynthesis may be assessed at the river reach scale using an open channel diel change in oxygen method. We developed a new model integrating and expanding the whole stream metabolism approach (Odum, 1956) with a modified flow routing model similar to Sincock and Lees (2002) to estimate plant gross primary production. The observed net ecosystem production (NEP, g O_2 m^{-2} min^{-1}) at time *t* was estimated with an accounting two-station open channel method (Pathak and Demars, 2023), as follows:

$$NEP_t = \left(\frac{C_{t+\Delta t} - C_t}{\Delta t} - \frac{Q_{i,t-\alpha}}{Q_t \times T_{sadv}}\left(C_{i,t-\alpha} - C_t\right) - k\left(C_{s,t} - C_t\right)\right) z_t \qquad (1)$$

and

$$\alpha = F_{adv} \times T_{sadv} \qquad (2)$$

C_t, oxygen concentration at time *t* (mg O_2 L^{-1} or g O_2 m^{-3}), Δt time interval (15 min), C_s saturated oxygen concentration (mg O_2 L^{-1} or g O_2 m^{-3}), $Q_{i,t-\alpha}$ incoming discharge at the top of the reach (m^3 min^{-1}) at

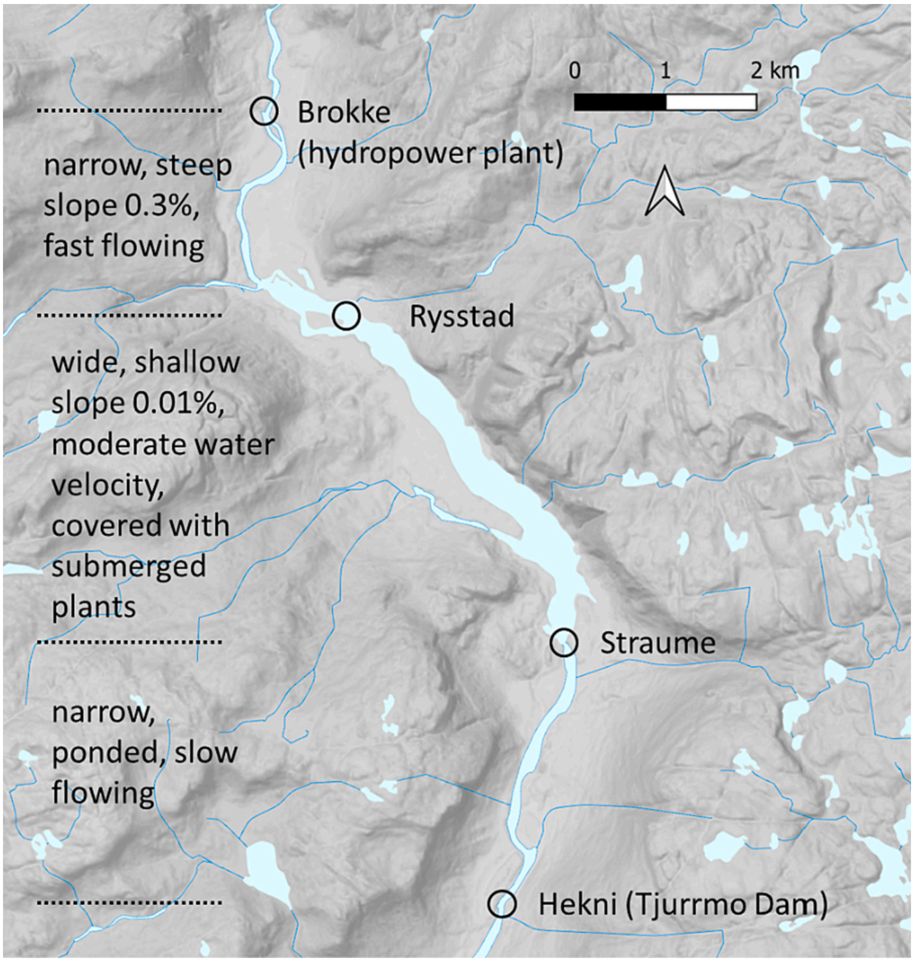

Fig. 1. Study area with three contrasting river sections. River flows from Brokke to Hekni. The hydropower plant effluent is at Brokke and the dissolved oxygen sensors were placed at Rysstad (top station) and Straume (bottom station). There is a dam at Hekni controlling the water level at least up to Straume.

time $t-\alpha$, α advection delay (min), F_{adv} advection coefficient (unitless, range 0–1), T_{sadv} mean solute travel time (min), Q_t outgoing discharge at the bottom of the river reach (same unit as Q_i), k gas exchange rate (min^{-1}), $C_{i,t-\alpha}$ incoming oxygen concentration (mg O$_2$ L^{-1} or g O$_2$ m^{-3}) at time $t-\alpha$, C_t outgoing oxygen concentration at time t, and z_t average stream water depth (m).

Gross primary production (GPP, g O$_2$ m^{-2} min^{-1}) was derived from

$$NEP_t = GPP_t - ER_t \tag{3}$$

where ER is ecosystem respiration (g O$_2$ m^{-2} min^{-1}), which was estimated during the night hours and assumed to be constant throughout the day. Note that ER is not reported in this study as it was still biased by supersaturation from the hydropower plant with ER linearly related to daily average TDG ($R^2 = 0.85$). The bias was possibly due to a weak independence (14 %) of the bottom station relative to the top station, with reach respiration estimates masked by difficulties in removing the effect of upstream processes (Demars et al., 2015). The supersaturation effect has recently been corrected through the use of TDG, travel time and gas exchange rate (Roley et al., 2023). Alternatively, the concomitant use of argon, a noble gas with similar diffusion and solubility to oxygen, allows the estimation of unbiased ER using only one station (Demars and Dörsch, 2023).

The model was parameterised as in Pathak and Demars (2023). Water depth z (range 1.3–2.4 m) was deduced through combination of a bathymetric survey, water level monitoring and discharge at Straume. Discharge at Rysstad and Straume were derived from a flow routing model calibrated with the two gauging stations (Brokke and Hekni), see Pathak and Demars (2023) for more details. Velocity ranged from 0.05 to 0.82 m s^{-1}. The gas exchange coefficient $k = 0.36$ day^{-1} was estimated using floating flux chambers (Bastviken et al., 2015) and was found to be independent of water temperature and discharge or depth (Pathak and Demars, 2023). The advection coefficient (unitless) was kept as $F_{adv} = 0.83$.

Calculations were done in Excel (Microsoft) assuming that measurement errors of the four key parameters were normally distributed. Uncertainties were propagated using 1000 Monte Carlo simulations. Uncertainties (standard deviation) were 0.1 mg O$_2$ L^{-1} for the oxygen concentrations, 0.07 day^{-1} for the gas exchange rate and 0.05 for the advection coefficient. In addition, discharge was allowed to vary within ±10 % error, the same error being used for Rysstad and Straume for each MC simulation, as discharge was derived from the same flow routing model also determining travel time and depth. We only retained results when TDG daily average in the effluent of the hydropower plant was within 90–130 %, the TDG standard deviation during the day was within 10 % and when the maximum TDG within a day did not exceed 140 % (to avoid periods of fizzing water within the studied reach). The 1000 simulations for the whole year took about 22 min on a laptop computer with 16 GB installed RAM (Intel® Core™ i5-6440HQ CPU @ 2.60GHz). The raw data and calculation spreadsheets are provided as Supplementary information.

2.3. Prediction of daily aquatic plant photosynthesis

The thermodynamic theory of enzyme kinetics can be simplified to an Arrhenius model of temperature dependence within the physiological temperature range (4–45 °C; Demars et al., 2016). We centred the temperature response function at $T_C = 283\,K = 10^\circ C$ similarly to Gillooly et al. (2001):

$$GPP_T = GPP_{TC}\,exp\left[E_a\left(\frac{1}{kT_C}-\frac{1}{kT}\right)\right] \tag{4}$$

with GPP_T and GPP_{TC} being gross primary production (g O$_2$ m^{-2} day^{-1}) at temperature T and centred temperature T_C, respectively, E_a activation energy of autotrophs (0.57 eV), and k Boltzmann constant (8.62 10^{-5} eV K^{-1}). In order to model light independently of temperature, the same equation (but inverting T and T_C) was first used to standardise the observed GPP_T to GPP at 10 °C (GPP_{TC}) and then regress GPP_{TC} against light using a Michaelis-Menten equation:

$$GPP_{TC} = \frac{GPPmax_{TC}\;PAR}{k_{PAR}+PAR} \tag{5}$$

with $GPPmax_{TC}$ being the maximum GPP at 10 °C, and PAR photosynthetic active radiation (mol quanta m^{-2} day^{-1}), and k_{PAR} the PAR at which half the $GPPmax_{TC}$ is realised. $GPPmax_{TC}$ and k_{PAR} were fitted parameters using a non-linear regression model in R (R Core Team, 2020).

Thus, the full predictive model with independent light and temperature effect was:

$$GPP_T = \frac{GPPmax_{TC}\;PAR}{k_{PAR}+PAR}\,exp\left[E_a\left(\frac{1}{kT_C}-\frac{1}{kT}\right)\right] \tag{6}$$

Observed GPP was then regressed against the predictive model to determine the proportion of variance explained by the model.

2.4. Prediction of photosynthesis recovery following aquatic plant harvesting

The above theory can make predictions for warming when the system is near equilibrium (or peak plant mass). In many cases the system will deviate significantly from equilibrium, particularly in the case of introduction of an invasive species, mechanical harvesting or annual plants. Plant colonisation rate may be modelled with a logistic growth curve as follows:

$$\frac{dB}{dt} = \frac{rB\left(B_{eq}-B\right)}{B_{eq}} \tag{7}$$

where B is plant biomass (g C m^{-2}) at time t, B_{eq} is plant biomass (g C m^{-2}) at equilibrium, and r plant expansion rate (day^{-1}).

The above equation can be generalised to modelling the proportion of biomass relative to equilibrium with $x = B/B_{eq}$ and we now have:

$$\frac{dx}{dt} = rx(1-x) \tag{8}$$

with solution:

$$x_t = \frac{1}{1+\left(\frac{1}{x_0}-1\right)e^{-rt}} \tag{9}$$

If we assume plant photosynthesis to be linearly dependent on biomass then we set

$$GPP_{T,t} = x_t\,\frac{GPPmax_{TC}\;PAR}{k_{PAR}+PAR}\,exp\left[E_a\left(\frac{1}{kT_C}-\frac{1}{kT}\right)\right] \tag{10}$$

Now we can study how GPP changes with varying x_0 representing *e.g.*, the efficiency of mechanical harvesting (% removal of biomass) and varying r representing *e.g.*, how fast an invasive species recolonises following harvesting. Here, we inferred r from removal experiments in the regulated River Mandalselva (Johansen, 2002), flowing parallel to the River Otra with similar environmental characteristics (Moe and Demars, 2017). Johansen et al. (2000) and Johansen (2002) reported three experiments: 72 % plant removal by machine and 99 % plant removal by hand in 50 m^2 and 100 m^2 plots, all done in 1996. The mechanical plant removal time series was re-aligned to have corresponding plant cover (28 % cover in 1996 for mechanical removal and average 27 % plant cover in 1998 for removal by hand). These data allowed to infer the expansion rate per year, which we converted in per day, and implicitly assumed to be valid at our centred temperature $T_C = 10^\circ C$. Note, plant expansion is also likely to be driven by temperature dependent processes which would combine multiplicatively and increase the apparent activation energy (Anderson-Teixeira et al., 2008).

In order to better visualise the results, we used *potential* daylight availability and a sine function for temperature while keeping the observed range and time lag in light and temperature of our study site. Daily PAR was determined from daylength (*D*, hours) using the StreamMetabolism package in R 4.0.0. (R Core Team, 2020; Sefick Jr., 2016) with the following empirical equation: $PAR = (D - 6.09) \times 3.73$ to fit the observed PAR fluctuation at our study site. The daily temperature at the *J* day of year (T_J) was modelled with a sine function: $T_J = 7 + 5.5\left[sin\frac{2\pi(-165+J)}{365}\right]$ to correspond with observed data. In our dataset, the first day of the year was December 1st. We set $x_0 = 0.01$ (corresponding to the 1 % cover or 99 % removal in the hand removal experiments) to infer the parameter *r* from a non-linear regression model in R (R Core Team, 2020). We also run the non-linear regression model with x_0 as free parameter to see how the estimation of *r* may be affected.

In June 2020, *J. bulbosus* was harvested mechanically in about 2 % of the Rysstad basin (Schneider et al., 2022). This had a negligible effect on dissolved oxygen at Straume, but provided a test dataset of plant regrowth. Plant biomass (roots and shoots) was estimated from 0.12 m^2 quadrats laid on patches of *J. bulbosus* before-after mechanical harvesting in control and impacted areas ($n = 20$, June 2020). Plant patch height and plant cover were estimated from point records along transects in both the control and impacted areas, before and after plant mechanical removal in June 2020 (see Schneider et al., 2022). The efficiency of harvesting was quantified as average standing biomass (patch biomass x plant cover) or average biovolume (patch height x plant cover, L m^{-2}). Monitoring post harvesting was only continued with biovolume.

3. Results

Large peaks of total dissolved gases (TDG), up to >200 % were observed in the hydropower plant effluent throughout the year (Fig. 2), independently of discharge (Fig. 3). The TDG supersaturation events were mirrored by the oxygen concentrations (Fig. 2). There were also periods throughout the year with no TDG supersaturation and more stable TDG. River water temperature was largely unrelated to light availability (Fig. 4). The average GPP (straight calculations) was highly related to the median GPP calculated stochastically by random Monte Carlo simulations (Fig. 5).

Gross primary production was much better related to light after taking into account the effect of temperature yielding a $GPPmax_{TC}$ value of 3.62 ± 0.07 g O_2 m^{-2} day^{-1} and a k_{PAR} value of 1.67 ± 0.18 mol quanta m^{-2} day^{-1} (Fig. 6). The full light-temperature model explained 87 % of the variance in observed GPP with a slope of 1.02 ± 0.01 (Fig. 7). The use of alternative temperature dependence over or under predicted observed GPP. Notably, using the temperature dependence of C3 plant metabolism (0.32 eV) underpredicted observed GPP by 12 ± 1 %. The model also fitted GPP observed during large supersaturation events (with TDG 140–180 %) using an O_2:Ar ratio method to isolate biological processes (metabolism) from purely physical supersaturation produced by the hydropower plant (Fig. 7, Demars and Dörsch, 2023).

From the three published *J. bulbosus* removal experiments and following re-growth (1996–2000), we were able to infer an expansion rate (±se) $r = 1.41 \pm 0.10$ $year^{-1}$ with $x_0 = 0.01$ ($R^2 = 0.54$) or $r = 1.06 \pm 0.33$ when x_0 was set as a free parameter, with inferred $x_0 = 0.03 \pm 0.03$ ($R^2 = 0.50$, Fig. 8). We used $r = 1.41$ for our plant removal simulations (Fig. 9). The simulations suggest that *J. bulbosus* would regrow rapidly following 50–85 % removal, while near total removal (99 %) would keep photosynthesis below 50 % of its capacity at equilibrium for three years (Fig. 9). The model provided general system behaviour, and on-going monitoring in the Rysstad basin showed *J. bulbosus* to recover within two years following plant mechanical removal in June 2020 of 72 ± 17 % biomass or 84 ± 6 % biovolume (±se) – see Fig. 9.

4. Discussion

4.1. Light and temperature controls on photosynthesis

Our results suggest that a simple model with just two independent drivers (light and temperature) was sufficient to model GPP in the River Otra. This is likely because neither the standing biomass of *J. bulbosus* nor key nutrients (CO_2, dissolved inorganic N, soluble reactive P) changed much throughout the year (Moe and Demars, 2017), suggesting that the Otra ecosystem was at or near steady-state. GPP was previously found to be independent of temperature *in spring* (O'Gorman et al., 2012) under the same light conditions for which the activation energy E_a was determined *under summer near steady-state conditions* (Demars et al., 2011; Demars et al., 2016). The lack of GPP response to temperature *in spring* was likely due to differences in standing biomass between spring and summer (see Gudmundsdottir et al., 2011) and could reconcile the lack of mass-specific GPP response to temperature found *in spring* without invoking additional temperature compensation mechanisms (as used by Padfield et al., 2017). The value for activation energy $E_a = 0.57$ eV was determined from a large set of streams independently of numerous other factors including standing biomass, nutrients, hydrology and top-down controls (Demars et al., 2016).

The apparent response of GPP to temperature may be inflated through interactions with limiting nutrients (Anderson-Teixeira et al., 2008; Cross et al., 2022; Cross et al., 2015). Determining the temperature dependence of GPP in streams empirically through inverse modelling across biomes, Song et al. (2018) reported a median similar to that used here (Demars et al., 2016), but also showed that individual *apparent* activation energy varied widely between streams (Song et al., 2018). The wide range of E_a values suggests that the temperature dependence was interacting with other factors, as reported extreme values have no direct physiological meaning. The challenge remains to identify those interactions more explicitly *a priori*. Metabolic theory allows to make *a priori* predictions on the role of temperature in ecosystems (Gillooly

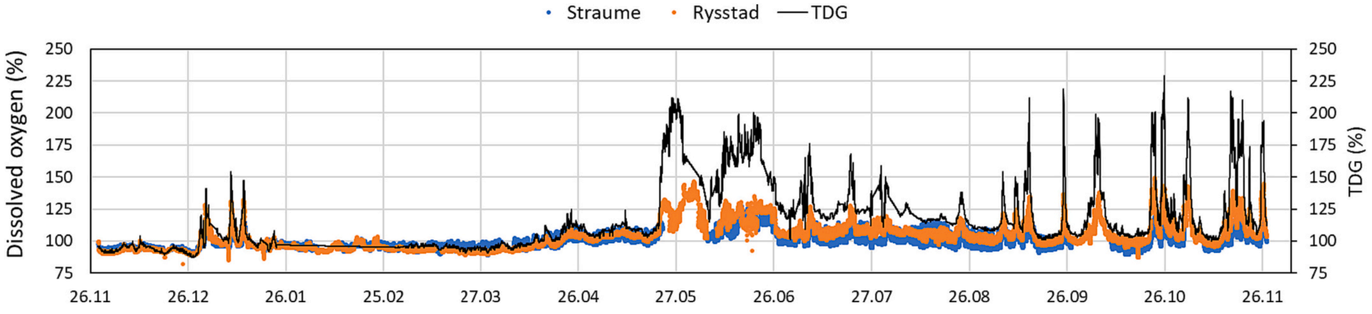

Fig. 2. Dissolved oxygen saturation (%) at Rysstad (top of the reach, orange dots) and Straume (bottom of the reach, blue dots); and total dissolved gases saturation (TDG, %, black line) during the annual cycle (Dec 2019-Nov 2020).

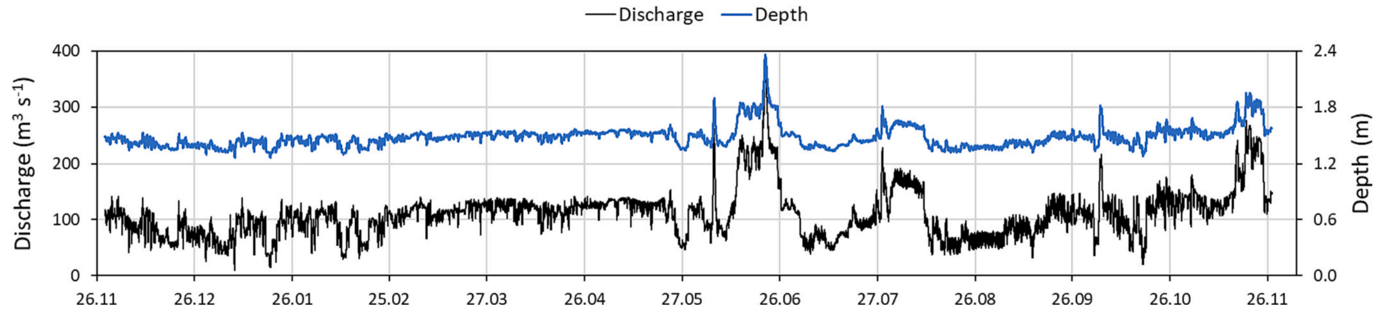

Fig. 3. Measured discharge (black line) at Hovet (3.5 km upstream the studied reach) and associated changes in river water depth (blue line) within the studied reach Rysstad-Straume during the annual cycle (Dec 2019-Nov 2020).

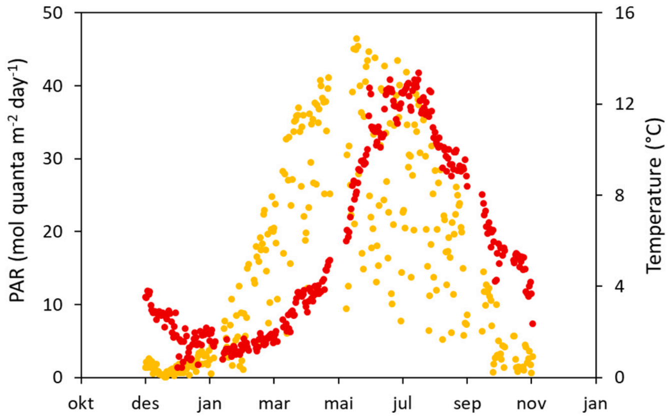

Fig. 4. River Otra decoupling of light availability (yellow points) and temperature (red points) during an annual cycle (December 2019–November 2020).

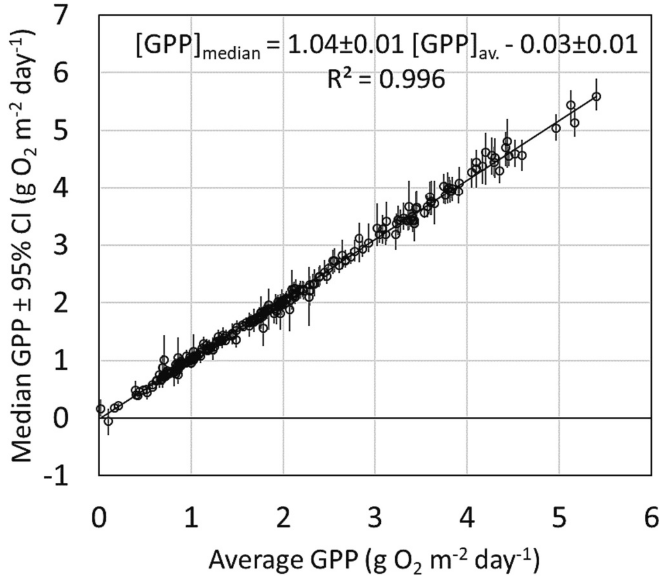

Fig. 5. Average gross primary production (GPP) highly related to GPP determined by Monte Carlo simulations (GPP median ± 95 % confidence interval).

et al., 2001; Anderson-Teixeira et al., 2008; O'Gorman et al., 2016). With rapid climate change, metabolic traits, such as E_a, could undergo modifications through evolutionary processes (Padfield et al., 2016; Thomas et al., 2012). Moreover, certain phylogenetic groups or individual species may exhibit varying rates of response to warming, with some adapting more quickly than others (Galmés et al., 2015; Barton and Yvon-Durocher, 2019).

Since we measured light (PAR) above the water surface, light availability could be varying with water depth and turbidity (Hall Jr. et al., 2015). The water of the River Otra remains very clear throughout the year. Turbidity (mean ± stdev) under low flows was below 1 NTU (0.7 ± 0.1 NTU; July 2020) and turbidity during the hydrological peak due to snowmelt remained low (3.5 ± 2.1 NTU; June 2020). Unsurprisingly, water depth was not related to the residual of the model. The standing biomass of *J. bulbosus* also seemed resilient to hydropeaking and 'dampened' snow melt events in the River Otra, in contrast to the green algae of the River Colorado studied by Hall Jr. et al. (2015).

4.2. Management

The plant removal scenarios suggested that photosynthetic capacity of *J. bulbosus* at equilibrium was recovered within two years of mechanical harvesting in the range 50–85 % removal, and that near total removal (99 %) was necessary to keep photosynthesis below 50 % of its capacity for three years. Such high removal efficiency would likely be prohibitively expensive. The results of the scenarios were similar with the lower expansion rate $r = 1.06$ year^{-1}. Note our net expansion rate of *J. bulbosus* based on field experiments were one or two orders of magnitude smaller than net growth rate reported in laboratory experiments (Wortelboer, 1990), so care should be taken in coupling demography and physiology (Vermaat and Verhagen, 1996). The independent field experiment from Rysstad basin confirmed the relevance of our scenarios for management.

General symptoms of water regulations may be mitigated through flow regime management (Palmer and Ruhi, 2019; Maavara et al., 2020; Sabo et al., 2017) and process-based restoration of fluvial geomorphology (Beechie et al., 2010; Ciotti et al., 2021). Here, in the River Otra, significant removal of plant biomass (30 % cover) was achieved through lowering the water level in mid-winter (−10 °C) for five days to freeze the river bed followed by increasing discharge from 2 to 150 m^3 s^{-1} within an hour (Rørslett and Johansen, 1996). However, *J. bulbosus* root system remained, the plant regrew rapidly, and the cost was prohibitive to the hydropower company (Rørslett and Johansen, 1996). Thus, mechanical harvesting along one side of the river has been the preferred management option. The cost of plant removal should, however, be carefully considered against the benefit of plant growth. For example, aquatic plants may reduce total dissolved gas in the water column by increasing the rate of bubble formation and gas evasion rate to the atmosphere (Yuan et al., 2018), potentially protecting fish from dissolved gas supersaturation (Lennox et al., 2022; Stenberg et al., 2022).

4.3. Ecological relevance for environmental policy

The EU Biodiversity Strategy for 2030 calls for developing an EU-wide methodology to map, assess and achieve good condition of

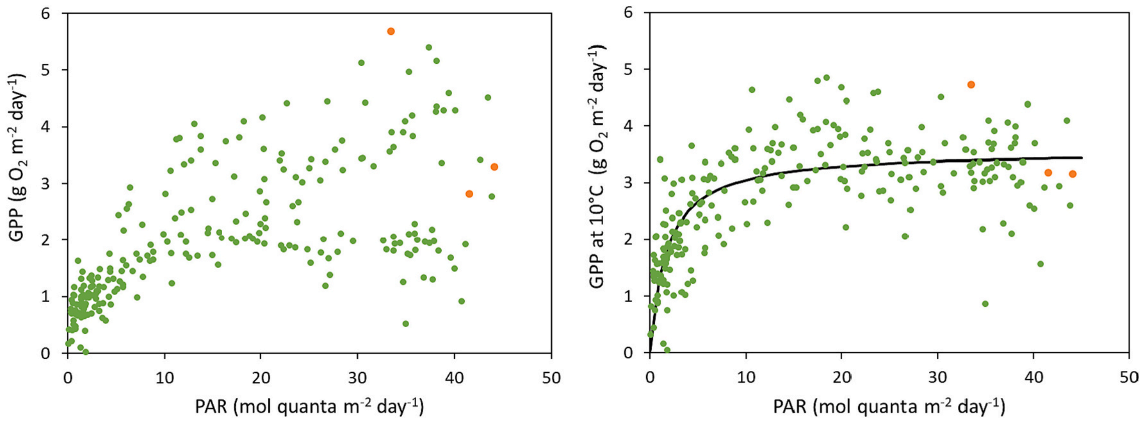

Fig. 6. Daily gross primary production (GPP) as a function of light (photosynthetic active radiation, PAR) without (left) and with (right) a temperature correction. The curve is a Michaelis-Menten type model fitted to daily GPP at 10 °C. The three datapoints in orange were determined with the O_2:Ar method.

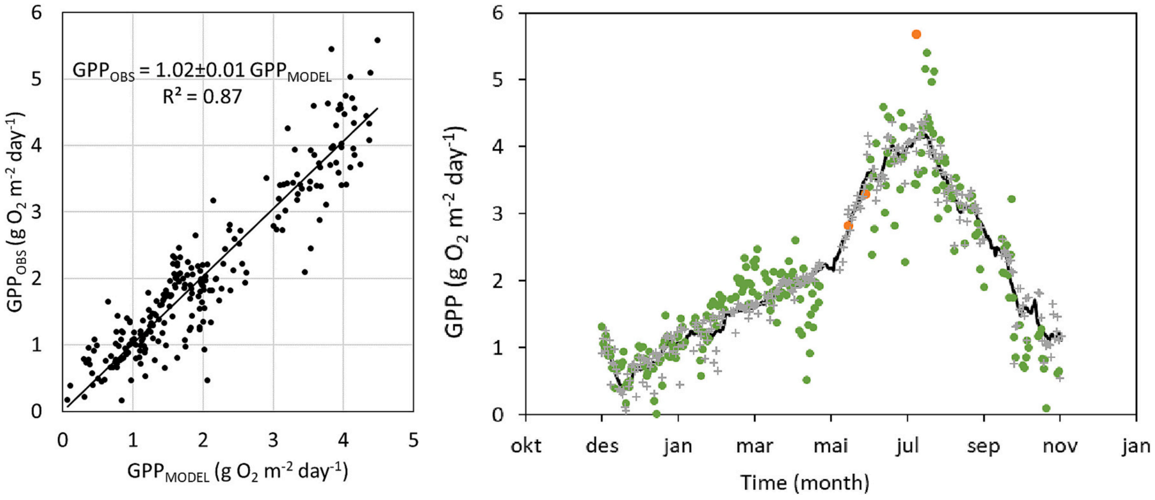

Fig. 7. Observed gross primary production (GPP_{OBS}) can be accurately predicted from a light and temperature model (GPP_{MODEL}; left graph). The GPP model (grey cross with moving average black line) could depict the daily observed GPP changes (green dot) throughout the year (right graph). The three datapoints in orange were determined with the O_2:Ar method.

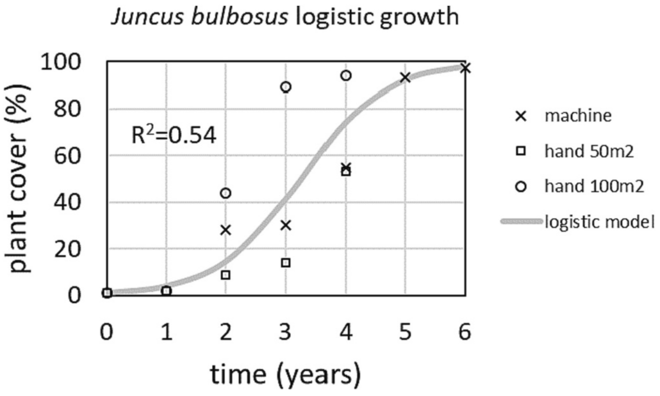

Fig. 8. Changes in plant cover (net growth) following mechanical harvesting to infer plant expansion rate (*r*).

ecosystems, so they can deliver benefits to society through the provision of ecosystem services (Vallecillo et al., 2022). The European habitats for freshwater ecosystems follow the EU Water Framework Directive (WFD, 2000/60/EC). The WFD defines ecological status as an expression of the quality of the structure and functioning of aquatic ecosystems associated with surface waters (Art. 2.21.), but current approaches generally rely on linking environmental pressures to taxonomic-based indices (Demars et al., 2012). The quantification of ecological functions, such as aquatic photosynthesis is more directly transferable to ecosystem services, such as carbon capture (regulating service).

The knock-on effect of barriers and water regulation on aquatic plant mass development and river functioning is poorly known, notably on food-web and carbon cycle (Battin et al., 2023; Ruhi et al., 2016; Jones et al., 2020). There is a pressing need to better understand the interactions between flow regime, biota and ecosystem processes (Palmer and Ruhi, 2019; Demars et al., 2021; Diamond et al., 2022). If we are to scale up our model from river reach to river network, we need to develop stronger predictive links with fluvial geomorphology and hydrology constraining standing biomass and metabolism (Junker et al., 2021; Gurnell, 2014; Warnaars et al., 2007). Novel GIS applications combining high resolution and large extent may help scaling up model results, *e.g.* potential sediment load and sediment trapping index (Grill et al., 2019).

Our study of the effect of mechanical plant removal and subsequent re-growth resonates with ongoing attempts to infer ecosystem resilience in response to flow disturbance (Blaszczak et al., 2023). The use of sensors with high frequency recording opens new opportunities to study rapid recolonisation or changes in metabolism following disturbance, often unattainable using traditional approaches to estimate river functioning, such as leaf litter decomposition (*in-situ* but takes weeks),

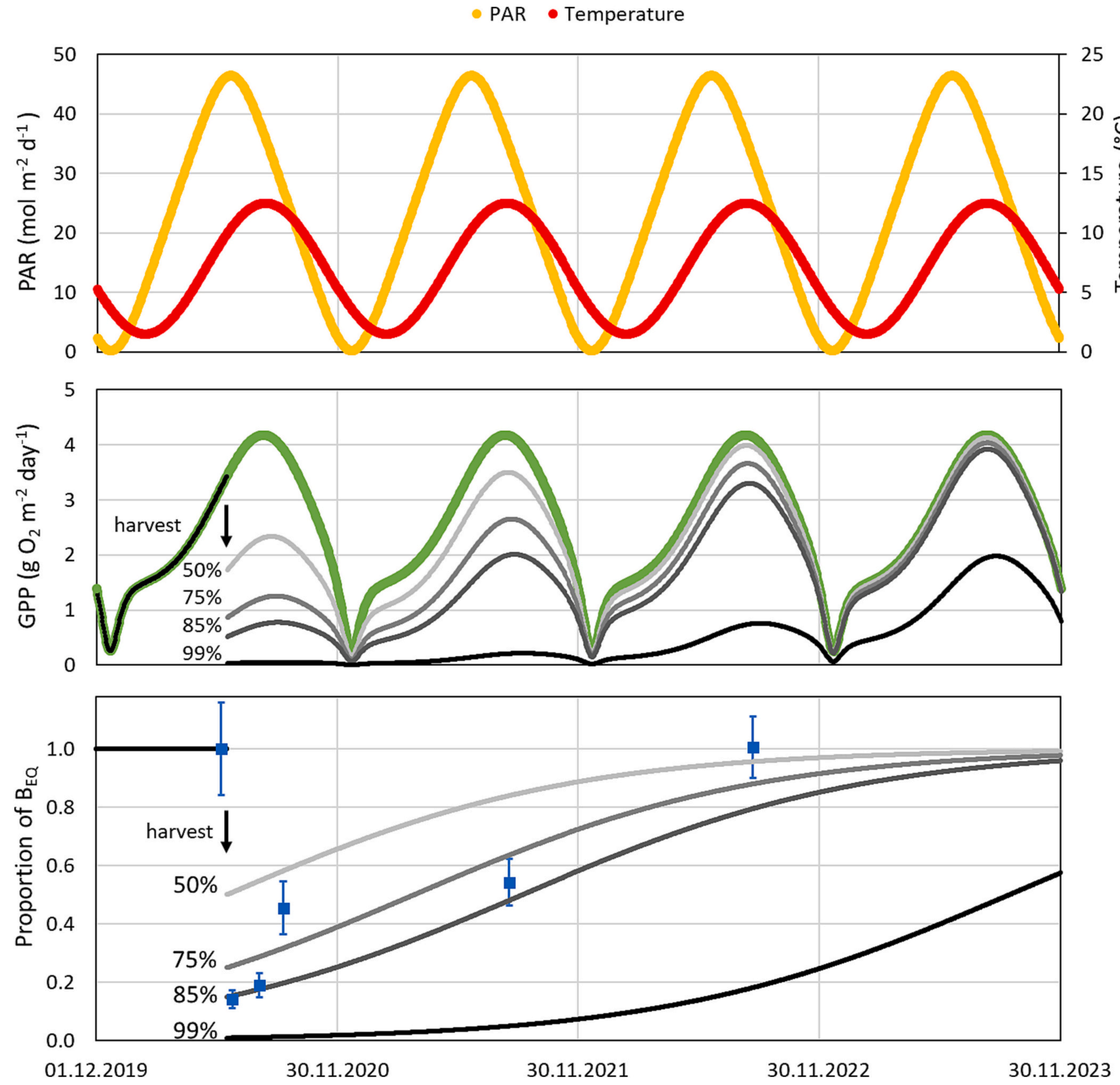

Fig. 9. Changes in gross primary production (GPP, green line) and proportion of biomass at equilibrium B_{eq} (black lines) derived from light-temperature model with scenarios of plant harvest (50–99 %). Blue squares with standard errors illustrate observed proportional changes in plant biovolume in area affected by mechanical removal in June 2020 (2 % of the area of Rysstad basin).

metabolic chambers or bottle incubations (discontinuous and labour intensive).

Here, the sum of GPP throughout the year was 271 g C m^{-2} $year^{-1}$, assuming a respiratory quotient of one. If we assume that 50 % (range 20–80 %) of GPP is lost through autotrophic respiration (Demars et al., 2015), then net primary production is 135 (54–217) g C m^{-2} $year^{-1}$. The annual growth of *J. bulbosus* was therefore 2.4 (1.0–3.8) times the average standing biomass of *J. bulbosus* over the reach (57 ± 8 g C m^{-2}). This suggests some continuous plant mass loss through hydraulic stress and natural mechanical break of stems (Dawson, 1976; Dawson, 1980). Plant photosynthesis contributes to regulate carbon fluxes in rivers and should be better incorporated into river C cycle and transferred into aquatic ecosystem services.

5. Conclusion

The photosynthetic rate of *J. bulbosus* throughout the year in the River Otra could be determined from a simple light-temperature model. More studies should consider theoretical approaches in applied ecology with *a priori* predictions, because empirical statistical analyses with *a posteriori* results are not always easy to interpret. Our ability to predict aquatic plant photosynthesis under varying climate and management scenarios provides the means to integrate river functions into the assessment of aquatic ecosystem services. This is particularly relevant to major policies such as the EU Biodiversity Strategy and the UN Sustainable Development Goals, where ecosystem services play a central role.

Supplementary data to this article can be found online at https://doi.

org/10.1016/j.scitotenv.2023.169201.

CRediT authorship contribution statement

Benoît O.L. Demars: Conceptualization, Data curation, Formal analysis, Funding acquisition, Methodology, Project administration, Visualization, Writing – original draft, Writing – review & editing. **Susanne C. Schneider:** Conceptualization, Funding acquisition, Investigation, Methodology, Project administration, Resources, Writing – review & editing. **Kirstine Thiemer:** Conceptualization, Investigation, Writing – review & editing. **Peter Dörsch:** Conceptualization, Data curation, Funding acquisition, Methodology, Writing – review & editing. **Ulrich Pulg:** Conceptualization, Investigation, Methodology, Writing – review & editing. **Sebastian Stranzl:** Conceptualization, Investigation, Methodology, Writing – review & editing. **Gaute Velle:** Conceptualization, Funding acquisition, Project administration, Writing – review & editing. **Devanshi Pathak:** Conceptualization, Methodology, Writing – review & editing.

Declaration of competing interest

The authors declare that they have no known competing financial interests or personal relationships that could have appeared to influence the work reported in this paper.

Data availability

We have made the data and calculations available in supplementary material

Acknowledgements

We thank Gjermund Espetveit (Otra Kraft) and Ole Morten Egeland (Agder Energy) for providing flow data; Torstein Try for providing the boats; Odd Arne Skogan for setting up the Campbell logging station; Leonhard B. Jansen for changing and recharging the batteries of the logging station; Knut Olav Oppstad for providing sonar bathymetric data; Emmanuel Bergan, Astrid Torske, Eirin Aasland for help collecting water samples, bathymetric and plant data, as well as CO_2 flux with the floating chambers. SSC, KT and BOLD gratefully acknowledge the Research Council of Norway (297202/E10), the German Federal Ministry of Education and Research (033WU005), the French Agence National de Recherche (N°ANR-18-IC4W-0004-06), the South African Water Research Commission (K5/2951) and Fundação Araucária in Brazil (N°186/2019) for funding of MadMacs (Mass development of aquatic macrophytes - causes and consequences of macrophyte removal for ecosystem structure, function, and services) in the frame of the collaborative inter-national consortium of the 2017 call of the Water Challenges for a Changing World Joint Programme Initiative (Water JPI). Additional funding was provided by Krypsivprosjektet på Sørlandet, the Norwegian Institute For Water Research (NIVA), the Research Council of Norway through the project SUPERSAT (294742), and the European Union's Horizon 2020 research and innovation programme under the Marie Skłodowska-Curie grant agreement no. 765553.

References

Allen, A.P., Gillooly, J.F., Brown, J.H., 2005. Linking the global carbon cycle to individual metabolism. Funct. Ecol. 19, 202–213.

Anderson-Teixeira, K.J., Vitousek, P.M., Brown, J.H., 2008. Amplified temperature dependence in ecosystems developing on the lava flows of Mauna Loa, Hawai'i. Proc. Natl. Acad. Sci. U. S. A. 105, 228–233.

Barton, S., Yvon-Durocher, G., 2019. Quantifying the temperature dependence of growth rate in marine phytoplankton within and across species. Limnol. Oceanogr. 64, 2081–2091.

Bastviken, D., Sundgren, I., Natchimuthu, S., Reyier, H., Galfalk, M., 2015. Technical note: cost-efficient approaches to measure carbon dioxide (CO2) fluxes and concentrations in terrestrial and aquatic environments using mini loggers. Biogeosciences 12, 3849–3859.

Battin, T.J., Lauerwald, R., Bernhardt, E.S., Bertuzzo, E., Gener, L.G., Hall Jr., R.O., Hotchkiss, E.R., Maavara, T., Pavelsky, T.M., Ran, L., 2023. River ecosystem metabolism and carbon biogeochemistry in a changing world. Nature 613, 449–459.

Beechie, T.J., Sear, D.A., Olden, J.D., Pess, G.R., Buffington, J.M., Moir, H., Roni, P., Pollock, M.M., 2010. Process-based principles for restoring river ecosystems. Bioscience 60, 209–222.

Bernhardt, E.S., Savoy, P., Vlah, M.J., Appling, A.P., Koenig, L.E., Hall, R.O., Arroita, M., Blaszczak, J.R., Carter, A.M., Cohen, M., Harvey, J.W., Heffernan, J.B., Helton, A.M., Hosen, J.D., Kirk, L., Mcdowell, W.H., Stanley, E.H., Yackulic, C.B., Grimm, N.B., 2022. Light and flow regimes regulate the metabolism of rivers. Proc. Natl. Acad. Sci. U. S. A. 119, e2121976119.

Blaszczak, J.R., Yackulic, C.B., Shriver, R.K., Hall, R.O., 2023. Models of underlying autotrophic biomass dynamics fit to daily river ecosystem productivity estimates improve understanding of ecosystem disturbance and resilience. Ecol. Lett. 26, 1510–1522.

Ciotti, D.C., Mckee, J., Pope, K.L., Kondolf, G.M., Pollock, M.M., 2021. Design criteria for process-based restoration of fluvial systems. Bioscience 71, 831–845.

Cross, W.F., Hood, J.M., Benstead, J.P., Huryn, A.D., Nelson, D., 2015. Interactions between temperature and nutrients across levels of ecological organization. Glob. Chang. Biol. 21, 1025–1040.

Cross, W.F., Hood, J.M., Benstead, J.P., Huryn, A.D., Welter, J.R., Gislason, G.M., Olafsson, J.S., 2022. Nutrient enrichment intensifies the effects of warming on metabolic balance of stream ecosystems. Limnol. Oceanogr. Lett. 7, 332–341.

Dawson, F.H., 1976. The annual production of the aquatic macrophyte *Ranunculus penicillatus* var. *calcareus* (R.W. Butcher) C.D.K Cook. Aquat. Bot. 2, 51–73.

Dawson, F.H., 1980. The origin, composition and downstream transport of plant material in a small chalk stream. Freshw. Biol. 10, 419–435.

Demars, B.O.L., 2019. Hydrological pulses and burning of dissolved organic carbon by stream respiration. Limnol. Oceanogr. 64, 406–421.

Demars, B.O.L., Dörsch, P., 2023. Estimation of ecosystem respiration and photosynthesis in supersaturated stream water downstream of a hydropower plant. Water Res. 247, 120842.

Demars, B.O.L., Manson, J.R., Olafsson, J.S., Gislason, G.M., Gudmundsdottir, R., Woodward, G., Reiss, J., Pichler, D.E., Rasmussen, J.J., Friberg, N., 2011. Temperature and the metabolic balance of streams. Freshw. Biol. 56, 1106–1121.

Demars, B.O.L., Potts, J.M., Trémolières, M., Thiébaut, G., Gougelin, N., Nordmann, V., 2012. River macrophyte indices: not the holy grail! Freshw. Biol. 57, 1745–1759.

Demars, B.O.L., Thompson, J., Manson, J.R., 2015. Stream metabolism and the open diel oxygen method: principles, practice, and perspectives. Limnol. Oceanogr. - Method 13, 356–374.

Demars, B.O.L., Gislason, G.M., Olafsson, J.S., Manson, J.R., Friberg, N., Hood, J.M., Thompson, J.J.D., Freitag, T.E., 2016. Impact of warming on CO_2 emissions from streams countered by aquatic photosynthesis. Nat. Geosci. 9, 758–761.

Demars, B.O.L., Friberg, N., Thornton, B., 2020. Pulse of dissolved organic matter alters reciprocal carbon subsidies between autotrophs and bacteria in stream food webs. Ecol. Monogr. 90, e01399.

Demars, B.O.L., Kemp, J.L., Marteau, B., Friberg, N., Thornton, B., 2021. Stream macroinvertebrates and carbon cycling in tangled food webs. Ecosystems 24, 1944–1961.

Diamond, J.S., Moatar, F., Cohen, M.J., Poirel, A., Martinet, C., Maire, A., Pinay, G., 2022. Metabolic regime shifts and ecosystem state changes are decoupled in a large river. Limnol. Oceanogr. 67, S54–S70.

Elias, M., Wieczorek, G., Rosenne, S., Tawfik, D.S., 2014. The universality of enzymatic rate-temperature dependency. Trends Biochem. Sci. 39, 1–7.

Galmés, J., Kapralov, M.V., Copolovici, L.O., Hermida-Carrera, C., Niinemets, Ü., 2015. Temperature responses of the rubisco maximum carboxylase activity across domains of life: phylogenetic signals, trade-offs, and importance for carbon gain. Photosynth. Res. 123, 183–201.

Gillooly, J.F., Brown, J.H., West, G.B., Savage, V.M., Charnov, E.L., 2001. Effects of size and temperature on metabolic rate. Science 293, 2248–2251.

Grill, G., Lehner, B., Thieme, M., Geenen, B., Tickner, D., Antonelli, F., Babu, S., Borrelli, P., Cheng, L., Crochetiere, H., Macedo, H.E., Filgueiras, R., Goichot, M., Higgins, J., Hogan, Z., Lip, B., Mcclain, M.E., Meng, J., Mulligan, M., Nilsson, C., Olden, J.D., Opperman, J.J., Petry, P., Liermann, C.R., Saenz, L., Salinas-Rodriguez, S., Schelle, P., Schmitt, R.J.P., Snider, J., Tan, F., Tockner, K., Valdujo, P. H., Van Soesbergen, A., Zarfl, C., 2019. Mapping the world's free-flowing rivers. Nature 569, 215–221.

Gudmundsdottir, R., Olafsson, J.S., Palsson, S., Gislason, G.M., Moss, B., 2011. How will increased temperature and nutrient enrichment affect primary producers in sub-Arctic streams? Freshw. Biol. 56, 2045–2058.

Gurnell, A., 2014. Plants as river system engineers. Earth Surf. Process. Landf. 39, 4–25.

Hall Jr., R.O., Yackulic, C.B., Kennedy, T.A., Yard, M.D., Rosi-Marshall, E.J., Voichick, N., Behn, K.E., 2015. Turbidity, light, temperature, and hydropeaking control primary productivity in the Colorado River, grand canyon. Limnol. Oceanogr. 60, 512–526.

Huryn, A.D., Benstead, J.P., Parker, S.M., 2014. Seasonal changes in light availability modify the temperature dependence of ecosystem metabolism in an arctic stream. Ecology 95, 2826–2839.

Hussner, A., Stiers, I., Verhofstad, M., Bakker, E.S., Grutters, B.M.C., Haury, J., Van Valkenburg, J., Brundu, G., Newman, J., Clayton, J.S., Anderson, L.W.J., Hofstra, D., 2017. Management and control methods of invasive alien freshwater aquatic plants: a review. Aquat. Bot. 136, 112–137.

Johansen, S.W., 2002. Tiltaksplan for fjerning av krypsiv i Otra gjennom Valle kommune. Norsk institutt for vannforskning, Oslo, 4579–2002. http://hdl.handle.net/11250/211836.

Johansen, S.W., Brandrud, T.E., Mjelde, M., 2000. Konsekvenser av reguleringsinngrep på vannvegetasjon i elver. Tilgroing med krypsiv. Kunnskapsstatus. Norsk Institute for Vannforskning, Oslo, 4321-2000. http://hdl.handle.net/11250/211107.

Jones, P.E., Consuegra, S., Borger, L., Jones, J., De Leaniz, C.G., 2020. Impacts of artificial barriers on the connectivity and dispersal of vascular macrophytes in rivers: a critical review. Freshw. Biol. 65, 1165–1180.

Junker, J.R., Cross, W.F., Benstead, J.P., Huryn, A.D., Hood, J.M., Nelson, D., Gislason, G.M., Olafsson, J.S., 2021. Flow is more important than temperature in driving patterns of organic matter storage and stoichiometry in stream ecosystems. Ecosystems 24, 1317–1331.

Lennox, R.J., Thiemer, K., Vollset, K.W., Pulg, U., Stranzl, S., Nilsen, C.I., Haugen, T.O., Velle, G., 2022. Behavioural response of brown trout (Salmo trutta) to total dissolved gas supersaturation in a regulated river. Ecohydrology 15, e2363.

Liess, A., Lange, K., Schulz, F., Piggott, J.J., Matthaei, C.D., Townsend, C.R., 2009. Light, nutrients and grazing interact to determine diatom species richness via changes to productivity, nutrient state and grazer activity. J. Ecol. 97, 326–336.

Maavara, T., Chen, Q.W., Van Meter, K., Brown, L.E., Zhang, J.Y., Ni, J.R., Zarfl, C., 2020. River dam impacts on biogeochemical cycling. Nature Rev. Earth Environ. 1, 103–116.

Misteli, B., Pannard, A., Aasland, E., Harpenslager, S.F., Motitsoe, S., Thiemer, K., Llopis, S., Coetzee, J., Hilt, S., Kohler, J., Schneider, S.C., Piscart, C., Thiebaut, G., 2023. Short-term effects of macrophyte removal on aquatic biodiversity in rivers and lakes. J. Environ. Manag. 325.

Moe T.F. & Demars B.O.L. (2017) Årsrapport krypsivovervåking 2017. NIVA. L.NR. 7202-2017 Oslo.

Nilsson, C., 1978. Changes in the aquatic flora along a stretch of the river Umeälven, N. Sweden, following hydro-electric exploitation. Hydrobiologia 61, 229–236.

Nilsson, C., Reidy, C.A., Dynesius, M., Revenga, C., 2005. Fragmentation and flow regulation of the world's large river systems. Science 308, 405–408.

Odum, H.T., 1956. Primary production in flowing waters. Limnol. Oceanogr. 1, 102–117.

O'gorman, E.J., Pichler, D.E., Adams, G., Benstead, J.P., Cohen, H., Craig, N., Cross, W. F., Demars, B.O.L., Friberg, N., Gislason, G.M., Gudmundsdottir, R., Hawczak, A., Hood, J.M., Hudson, L.N., Johansson, L., Johansson, M.P., Junker, J.R., Laurila, A., Manson, J.R., Mavromati, E., Nelson, D., Olafsson, J.S., Perkins, D.M., Petchey, O.L., Plebani, M., Reuman, D.C., Rall, B.C., Stewart, R., Thompson, M.S.A., Woodward, G., 2012. Impacts of warming on the structure and functioning of aquatic communities: individual to ecosystem level responses. Adv. Ecol. Res. 47, 81–176.

O'gorman, E.J., Olafsson, O.P., Demars, B.O.L., Friberg, N., Gudbergsson, G., Hannesdottir, E.R., Jackson, M.C., Johansson, L.S., Mclaughlin, O.B., Olafsson, J.S., Woodward, G., Gislason, G.M., 2016. Temperature effects on fish production across a natural thermal gradient. Glob. Chang. Biol. 22, 3206–3220.

Padfield, D., Yvon-Durocher, G., Buckling, A., Jennings, S., Yvon-Durocher, G., 2016. Rapid evolution of metabolic traits explains thermal adaptation in phytoplankton. Ecol. Lett. 19, 133–142.

Padfield, D., Lowe, C., Buckling, A., Ffrench-Constant, R., Jennings, S., Shelley, F., Olafsson, J.S., Yvon-Durocher, G., Student, Res T., 2017. Metabolic compensation constrains the temperature dependence of gross primary production. Ecol. Lett. 20, 1250–1260.

Palmer, M., Ruhi, A., 2019. Linkages between flow regime, biota, and ecosystem processes: implications for river restoration. Science 365, eaaw2087.

Pathak, D., Demars, B.O.L., 2023. Metabolism modelling in rivers with unsteady flow conditions and transient storage zones. J. Geophys. Res. Biogeosci. 128, e2022JG007245.

Pulg, U., Stranzl, S., Vollset, K.W., Barlaup, B.T., Olsen, E., Skår, B., Velle, G., 2016a. Gassmetning i Otra nedenfor Brokke kraftverk. Laboratorium for ferskvannsøkologi og innlandsfiske (LFI). UNI Research Miljø, Bergen. http://hdl.handle.net/11250/2628615.

Pulg, U., Vollset, K.W., Velle, G., Stranzl, S., 2016b. First observations of saturopeaking: characteristics and implications. Sci. Total Environ. 573, 1615–1621.

Pulg, U., Espedal, E.O., Enqvist, M., Stranzl, S., 2022. Gassmetning i Otra nedenfor Brokke 2020–2021. Uni Research Bergen. Rapport 454. Uni Research Miljø LFI. https://norceresearch.brage.unit.no/norceresearch-xmlui/.

R Core Team, 2020. R: A language and environment for statistical computing. http://www.R-project.org/, 31.07.2022.

Riis, T., Biggs, B.J.F., 2003. Hydrologic and hydraulic control of macrophyte establishment and performance in streams. Limnol. Oceanogr. 48, 1488–1497.

Roelofs, J.G.M., Schuurkes, J.a.a.R., Smits, A.J.M., 1984. Impact of acidification and eutrophication on macrophyte communities in soft waters. II. Experimental studies. Aquat. Bot. 18, 389–411.

Roley, S.S., Hall Jr., R.O., Perkins, W., Garayburu-Caruso, V.A., Stegen, J.C., 2023. Coupled primary production and respiration in a large river contrasts with smaller rivers and streams. Limnol. Oceanogr. 68, 2461–2475.

Rørslett, B., 1988. Aquatic weed problems in a hydroelectric river: the R. Otra, Norway. Regul. Rivers Res. Manag. 2, 25–37.

Rørslett, B., Johansen, S.W., 1996. Remedial measures connected with aquatic macrophytes in Norwegian regulated rivers and reservoirs. Reg. River-Res. Manage. 12, 509–522.

Rørslett, B., Mjelde, M., Johansen, J., 1989. Effects of hydropower development on aquatic macrophytes in Norwegian rivers: present state of knowledge and some case studies. Regul. Rivers Res. Manag. 3, 19–28.

Ruhi, A., Munoz, I., Tornes, E., Batalla, R.J., Vericat, D., Ponsati, L., Acuna, V., Von Schiller, D., Marce, R., Bussi, G., Frances, F., Sabater, S., 2016. Flow regulation increases food-chain length through omnivory mechanisms in a Mediterranean river network. Freshw. Biol. 61, 1536–1549.

Sabo, J.L., Ruhi, A., Holtgrieve, G.W., Elliott, V., Arias, M.E., Ngor, P.B., Räsänen, T.A., Nam, S., 2017. Designing river flows to improve food security futures in the Lower Mekong Basin. Science 358, eaao1053.

Sand-Jensen, K., 1987. Environmental control of bicarbonate use among freshwater and marine macrophytes. In: Crawford, R.M.M. (Ed.), Plant Life in Aquatic and Amphibious Habitats. Blackwell Scientific Publications, Oxford, pp. 99–112.

Schneider, S.C., Andersen, E.E., Mutinova, P.T., 2022. Gjenvekst av krypsiv etter tiltak, og effekter av kalking på krypsiv i Otra ved Rysstad. Norwegian Institute for Water Research, Oslo. Rapport 7733-2022.

Schultz, R., Dibble, E., 2012. Effects of invasive macrophytes on freshwater fish and macroinvertebrate communities: the role of invasive plant traits. Hydrobiologia 684, 1–14.

Sefick Jr., S., 2016. Stream metabolism-a package for calculating single station metabolism from diurnal oxygen curves. In: R package version 1.1.2. https://cran.r-project.org/package=StreamMetabolism.

Sincock, A.M., Lees, M.J., 2002. Extension of the QUASAR river-water quality model to unsteady flow conditions. J. Chartered Inst. Water Environ. Manage. 16, 12–17.

Song, C., Dodds, W.K., Rüegg, J., Argerich, A., Baker, C.L., Bowden, W.B., Douglas, M.M., Farrell, K.J., Flinn, M.B., Garcia, E.A., 2018. Continental-scale decrease in net primary productivity in streams due to climate warming. Nat. Geosci. 11, 415–420.

Stenberg, S.K., Velle, G., Pulg, U., Skoglund, H., 2022. Acute effects of gas supersaturation on Atlantic salmon smolt in two Norwegian rivers. Hydrobiologia 849, 527–538.

Thiemer, K., Schneider, S.C., Demars, B.O.L., 2021. Mechanical removal of macrophytes in freshwater ecosystems: implications for ecosystem structure and function. Sci. Total Environ. 782, 146671.

Thiemer, K., Immerzeel, B., Schneider, S., Sebola, K., Coetzee, J., Baldo, M., Thiebaut, G., Hilt, S., Kohler, J., Harpenslager, S.F., Vermaat, J.E., 2023. Drivers of perceived nuisance growth by aquatic plants. Environ. Manag. 71, 1024–1036.

Thomas, M.K., Kremer, C.T., Klausmeier, C.A., Litchman, E., 2012. A global pattern of thermal adaptation in marine phytoplankton. Science 338, 1085–1088.

Vallecillo, S., Maes, J., Teller, A., Babí, Almenar J., Barredo, J., Trombetti, M., Malak, A., 2022. EU-Wide Methodology to Map and Assess Ecosystem Condition, Towards a Common Approach Consistent with a Global Statistical Standard. Publications Office of the European Union, Luxembourg. https://doi.org/10.2760/13048. EUR 31226 EN.

Velle, G., Skoglund, H., Barlaup, B.T., 2022. Effects of nuisance submerged vegetation on the fauna in Norwegian rivers. Hydrobiologia 849, 539–556.

Verhofstad, M.J., Bakker, E.S., 2019. Classifying nuisance submerged vegetation depending on ecosystem services. Limnology 20, 55–68.

Vermaat, J.E., Verhagen, F.C.A., 1996. Seasonal variation in the intertidal seagrass Zostera noltii Hornem: coupling demographic and physiological patterns. Aquat. Bot. 52, 259–281.

Warnaars, T.A., Hondzo, M., Power, M.E., 2007. Abiotic controls on periphyton accrual and metabolism in streams: scaling by dimensionless numbers. Water Resour. Res. 43, W08425.

Weiss, R.F., 1970. The solubility of nitrogen, oxygen and argon in water and seawater. Deep-Sea Res. 17, 721–735.

Wetzel, R.G., Brammer, E.S., Forsberg, C., 1984. Photosynthesis of submersed macrophytes in acidified lakes. I. Carbon fluxes and recycling of CO2 in Juncus bulbosus L. Aquat. Bot. 19, 329–342.

Wetzel, R.G., Brammer, E.S., Lindstrom, K., Forsberg, C., 1985. Photosynthesis of submersed macrophytes in acidified lakes. II. Carbon limitation and utilization of benthic CO2 sources. Aquat. Bot. 22, 107–120.

Wortelboer, R., 1990. A model on the competition between two macrophyte species in acidifying shallow soft-water lakes in the Netherlands. Hydrol. Bull. 24, 91–107.

Wright, R.F., Couture, R.-M., Christiansen, A.B., Guerrero, J.-L., Kaste, O., Barlaup, B.T., 2017. Effects of multiple stresses hydropower, acid deposition and climate change on water chemistry and salmon populations in the river Otra, Norway. Sci. Total Environ. 574, 128–138.

Yuan, Y.Q., Feng, J.J., Li, R., Huang, Y.H., Huang, J.P., Wang, Z.H., 2018. Modelling the promotion effect of vegetation on the dissipation of supersaturated total dissolved gas. Ecol. Model. 386, 89–97.